a reprint from Applied Optics

Light scattering by size–shape distributions of randomly oriented axially symmetric particles of a size comparable to a wavelength

Michael I. Mishchenko

The $\mathcal{T}$-matrix method, as extended recently to randomly oriented scatterers [J. Opt. Soc. Am. A **8**, 871 (1991)], is used to calculate rigorously light scattering by size–shape distributions of randomly oriented axially symmetric particles. The computational scheme is described in detail along with a newly developed convergence procedure that enables one to substantially reduce computer time and storage requirements. It is demonstrated that the elements of the Stokes scattering matrix for a power law size distribution of randomly oriented moderately aspherical spheroids are much smoother than and differ substantially from those of equivalent monodisperse spheroids, and thus averaging over orientations does not eliminate the necessity of averaging over particle sizes. Numerical calculations are reported for volume-equivalent polydispersions of spheres and size–shape distributions of moderately aspherical spheroids with the index of refraction $1.5 + 0.02\,i$, which is typical of some maritime aerosols. The angular-scattering behavior of the ensembles of nonspherical particles is found to be greatly different from that of the equivalent polydisperse spheres. The size–shape distributions of spheroids exhibit stronger side scattering near 120° and weaker backscattering, the ratio F_{22}/F_{11} of the elements of the scattering matrix substantially deviates from unity, and the element F_{33} is greatly different from F_{44}. For size distributions of oblate and prolate spheroids of the same aspect ratio, the ratios F_{22}/F_{11}, F_{33}/F_{11}, and F_{34}/F_{11} can differ substantially and, thus, are indicators of particle shape, whereas the angular patterns of the intensity (F_{11}) and linear polarization ($-F_{12}/F_{11}$) are similar. For the size–shape distributions of moderately aspherical spheroids, the optical cross sections, the single-scattering albedo, and the asymmetry parameter of the phase function do not differ substantially from those of equivalent spheres. In general, the elements of the scattering matrix and optical cross sections are more shape dependent for larger particles.

Key words: Light scattering, polarization, nonspherical particles, ensemble averaging.

1. Introduction

Calculations of scattering of light by small particles are important in many diverse fields of science and engineering. In most cases of practical interest, scattering particles are nonspherical and are distributed over sizes, shapes, and orientations. However, accurate light-scattering computations for ensembles of nonspherical particles are difficult and time consuming, and the literature in which such calculations are reported is rather scarce (see, e.g., Refs. 1–5 and a review paper by Bohren and Singham[6]).

At present, the $\mathcal{T}$-matrix approach[7] (or the extended boundary condition method[8]) is, apparently, the most powerful tool for solving nonspherical scattering problems.[9,10] It is the aim of the present paper to apply the $\mathcal{T}$-matrix approach, as developed in Ref. 11, to calculate light scattering by size–shape distributions of randomly oriented rotationally symmetric particles and to study how light scattering depends on particle shape. Basic concepts of the computational scheme are outlined in Section 2. Because convergence problems are important in the $\mathcal{T}$-matrix computations, in Section 3 we describe a new convergence procedure that seems to be especially suited to the case of randomly oriented particles and may be considered a substantial supplement to the method developed in Ref. 11. In Section 4, numerical calculations for polydispersions of spheres and size–shape distributions of spheroids are pre-

The author is with NASA, Goddard Institute for Space Studies, Hughes STX Corporation, 2880 Broadway, New York, New York 10025.

Received 22 September 1992.
0003-6935/93/244652-15$06.00/0.
© 1993 Optical Society of America.

sented and compared. The main results of the paper are discussed and summarized in Section 5.

It should be noted here that comparison of the light-scattering properties of particles of different shape is only meaningful if the particles are equivalent in a certain sense. Although different definitions of particle equivalence may be found in the literature, in this paper we use the definition according to which particles of different shape are considered equivalent if they have the same volume. Therefore the main size characteristic of any nonspherical particle is the radius of the equal-volume sphere.

2. Basic Concepts

The single scattering of light by a small-volume element consisting of randomly oriented axially symmetric particles is completely specified by the cross sections for scattering, C_{sca}, and extinction, C_{ext}, and the elements of the normalized scattering matrix $\mathbf{F}$.[12,13] This matrix relates the Stokes vectors of the incident light, $\mathbf{I}_i$, and the scattered light, $\mathbf{I}_s$:

$$\mathbf{I}_s = \frac{C_{sca}}{4\pi R^2}\mathbf{F}(\vartheta)\mathbf{I}_i, \tag{1}$$

where R is the distance between the volume element and the observation point and ϑ is the scattering angle,

$$\mathbf{I}_s = \begin{bmatrix} I_s \\ Q_s \\ U_s \\ V_s \end{bmatrix}, \qquad \mathbf{I}_i = \begin{bmatrix} I_i \\ Q_i \\ U_i \\ V_i \end{bmatrix}, \tag{2}$$

$$\mathbf{F}(\vartheta) = \begin{bmatrix} F_{11}(\vartheta) & F_{12}(\vartheta) & 0 & 0 \\ F_{12}(\vartheta) & F_{22}(\vartheta) & 0 & 0 \\ 0 & 0 & F_{33}(\vartheta) & F_{34}(\vartheta) \\ 0 & 0 & -F_{34}(\vartheta) & F_{44}(\vartheta) \end{bmatrix}, \tag{3}$$

and the Stokes parameters I, Q, U, and V are defined with respect to the scattering plane, i.e., the plane through the incident and scattered beams.

In computations of both single and multiple light scattering, an efficient approach is to expand the elements of the scattering matrix as follows[14–17]:

$$F_{11}(\vartheta) = \sum_{s=0}^{s_{max}} a_1{}^s P_{00}{}^s(\cos\vartheta), \tag{4}$$

$$F_{22}(\vartheta) + F_{33}(\vartheta) = \sum_{s=2}^{s_{max}} (a_2{}^s + a_3{}^s) P_{22}{}^s(\cos\vartheta), \tag{5}$$

$$F_{22}(\vartheta) - F_{33}(\vartheta) = \sum_{s=2}^{s_{max}} (a_2{}^s - a_3{}^s) P_{2,-2}{}^s(\cos\vartheta), \tag{6}$$

$$F_{44}(\vartheta) = \sum_{s=0}^{s_{max}} a_4{}^s P_{00}{}^s(\cos\vartheta), \tag{7}$$

$$F_{12}(\vartheta) = \sum_{s=2}^{s_{max}} b_1{}^s P_{02}{}^s(\cos\vartheta), \tag{8}$$

$$F_{34}(\vartheta) = \sum_{s=2}^{s_{max}} b_2{}^s P_{02}{}^s(\cos\vartheta), \tag{9}$$

where $P^s_{mm}(\cos\vartheta)$ are generalized spherical functions[18] and the upper summation limit, s_{max}, depends on the desired accuracy of the computations. There are several reasons in favor of this approach.

1. If the expansion coefficients $a_1{}^s$ to $b_2{}^s$ are known, then the elements of the scattering matrix can easily be calculated for practically any number of scattering angles with a minimum expense of computer time. Thus instead of specifying the elements of the scattering matrix for a large number of scattering angles, one may use a limited (and usually small) number of numerically significant expansion coefficients. This also makes the expansion coefficients especially convenient in size–shape averaging.

2. The expansion coefficients, if known, enable one to easily calculate Fourier components of the phase matrix appearing in the equation of transfer of polarized light in plane-parallel, macroscopically isotropic media.[19–22]

3. The expansion coefficients are ideally suited for checking convergence of light-scattering computations. As was mentioned above, there are a limited number of significant coefficients, which completely specify the scattering matrix for all the scattering angles $\vartheta \in [0, \pi]$ and can easily be used in the convergence criterion. Second, the generalized spherical functions are normalized such that $|P_{mn}{}^s(\cos\vartheta)| \leq 1$ for any $\vartheta \in [0, \pi]$ and any integers s, m, and n. Therefore the absolute accuracy of computing the expansion coefficients will also specify the absolute accuracy of computing the elements of the scattering matrix via Eqs. (4)–(9) and the Fourier components of the phase matrix.

4. An efficient analytical method of computing the expansion coefficients for randomly oriented, monodisperse, axially symmetric particles has been developed recently.[11] Specifically we have shown that instead of computing numerically the orientationally averaged elements of the scattering matrix of monodisperse, randomly oriented particles by averaging results for scattering by a single particle with varying orientation, the expansion coefficients can be analytically expressed in some basic quantities that depend only on the size, shape, and refractive index of the scattering particle and do not depend on any angular variable. These basic quantities are the elements of the natural $\mathscr{T}$ matrix of the axially symmetric scatterer. It was found that this analytical method is much faster than the common method of numerical integration over particle orientations.

To calculate the ensemble-averaged quantities C_{sca}, C_{ext}, and $a_1{}^s$ to $b_2{}^s$, we must average the optical cross sections and expansion coefficients over all particle

shapes and sizes. For simplicity, we will assume that the particle ensemble consists of J particle shapes with $p_j (1 \le j \le J)$ being the probability of the jth shape, and particles of each shape are distributed over sizes according to the same size distribution $n(r)$ such that $n(r)\,\mathrm{d}r$ is the fraction of the particles with equal-volume-sphere radii between r and $r + \mathrm{d}r$ with $r \in [r_{\min}, r_{\max}]$. The ensemble-averaged quantities are now obtained from (cf. Ref. 5)

$$C_{\mathrm{sca}} = \sum_{j=1}^{J} p_j \int_{r_{\min}}^{r_{\max}} \mathrm{d}r n(r) C_{\mathrm{sca}}{}^{j}(r), \tag{10}$$

$$C_{\mathrm{ext}} = \sum_{j=1}^{J} p_j \int_{r_{\min}}^{r_{\max}} \mathrm{d}r n(r) C_{\mathrm{ext}}{}^{j}(r), \tag{11}$$

$$a_i{}^s = \frac{1}{C_{\mathrm{sca}}} \sum_{j=1}^{J} p_j \int_{r_{\min}}^{r_{\max}} \mathrm{d}r n(r) C_{\mathrm{sca}}{}^{j}(r) [a_i{}^s(r)]^j, \quad i = 1, \ldots 4, \tag{12}$$

$$b_i{}^s = \frac{1}{C_{\mathrm{sca}}} \sum_{j=1}^{J} p_j \int_{r_{\min}}^{r_{\max}} \mathrm{d}r n(r) C_{\mathrm{sca}}{}^{j}(r) [b_i{}^s(r)]^j, \quad i = 1, 2. \tag{13}$$

The absorption cross section C_{abs}, single-scattering albedo ϖ, and asymmetry parameter of the phase function g are defined as

$$C_{\mathrm{abs}} = C_{\mathrm{ext}} - C_{\mathrm{sca}}, \tag{14}$$

$$\varpi = C_{\mathrm{sca}}/C_{\mathrm{ext}}, \tag{15}$$

$$g = \frac{1}{2} \int_{-1}^{+1} \mathrm{d}(\cos \vartheta) F_{11}(\vartheta) \cos \vartheta = a_1{}^1/3. \tag{16}$$

To calculate the integrals appearing in Eqs. (10)–(13), we use a Gaussian quadrature formula. Thus the computation of the ensemble-averaged quantities includes the following steps. First the optical cross sections and the expansion coefficients are calculated, as described in Ref. 11, for each couple (j, n), where the index j numbers particle shapes and the index n numbers Gaussian quadrature division points on the interval $[r_{\min}, r_{\max}]$. Second the size–shape-averaged cross sections, expansion coefficients, single-scattering albedo, and asymmetry parameter of the phase function are calculated via Eqs. (10)–(16). The number of Gaussian points, N, is increased until the expansion coefficients converge within the desired absolute accuracy of the computations, Δ. An *a priori* estimate of N can be obtained by checking convergence of analogous computations for equal-volume spheres, because orientational averaging in itself is a smoothing process, and, therefore, the scattering behavior of monodisperse randomly oriented nonspherical particles is smoother than that of monodisperse spheres.[1] Indeed, our test calculations have shown that we do not need to consider more spheroidal than spherical sizes in size averaging. Finally the expansions (4)–(9) are used to calculate the elements of the ensemble-averaged scattering matrix for practically any number of scattering angles. Alternatively, the single-scattering albedo and the expansion coefficients may serve as input parameters for multiple-scattering calculations.[19–22]

Of course, it is possible to consider a continuous rather than a discrete distribution of particle shapes in Eqs. (10)–(13). In that case, the summations over the index j are replaced by integrations over parameters that specify particle shapes (e.g., the ratio of the semiaxes of a spheroid), a Gaussian quadrature formula may be used to evaluate all the integrals numerically, and a procedure like that described in the preceding paragraph should be used to check convergence of the computations over the number of Gaussian division points.

The computational scheme outlined implies that the optical cross sections and expansion coefficients are calculated for each ensemble member corresponding to a couple (j, n) by using the method developed by Ref. 11. The procedure described there is well suited for calculations on a case-by-case basis and for checking the convergence of the $\mathcal{T}$-matrix computations by hand. Because studying particle ensembles requires multiple repeated calculations, thus precluding the possibility of examining each ensemble member individually, developing an efficient automatic convergence procedure becomes an important task. In Section 3 we describe such an automatic convergence procedure, which may be considered a supplement to the method developed in Ref. 11.

3. Convergence Procedure

A. Convergence Over $n_{\max}$

In $\mathcal{T}$-matrix computations of light scattering by nonspherical particles, both the incident and scattered electric fields are expanded in vector spherical waves, and transformation of the expansion coefficients of the incident field into those of the scattered field is given by the so-called $\mathcal{T}$ matrix.[7–10] Theoretically these expansions are of infinite length and, thus, the $\mathcal{T}$ matrix is of infinite size. In practice, however, one has to truncate the $\mathcal{T}$ matrix after a finite number of leading, numerically significant elements. Therefore a special procedure should ge used to check convergence of the resulting solution over a computational parameter $n_{\max}$, which specifies the size of the $\mathcal{T}$ matrix.

Light-scattering computations based on the $\mathcal{T}$ matrix approach involve calculation of the $\mathcal{T}$ matrix as the first step and the use of this $\mathcal{T}$ matrix to calculate some scattering characteristics as the second step. In both steps, the same parameter $n_{\max}$ is usually used.[23–25] In other words, it is assumed that if one has to use a (large) parameter $n_{\max}$ to calculate accurately the $\mathcal{T}$ matrix, then the same parameter $n_{\max}$ should be used in the second step, i.e., all the calculated elements of the $\mathcal{T}$ matrix should be used in further light-scattering computations. We have

found, however, that at least for randomly oriented particles, two $n_{\max}$ parameters should be used instead. The first of them, $n_{\max}^1$, is used to calculate the $\mathscr{T}$ matrix, as described, e.g., in Refs. 23–25, and the second one, $n_{\max}^2 \leq n_{\max}^1$, is used in calculating the optical cross sections and expansion coefficients; the parameter $n_{\max}^2$ is often much smaller than $n_{\max}^1$. In other words, the parameter $n_{\max}^2$ determines the minimum upper part of the calculated $\mathscr{T}$ matrix that may be used in further computations without loss of accuracy. Thus it appears that a rather large parameter $n_{\max}^s$ may be required to calculate accurately even the leading elements of the $\mathscr{T}$ matrix, although only a few leading $\mathscr{T}$-matrix elements may be enough to calculate accurately the optical cross sections and expansion coefficients. Apparently this fact may be explained by the ill-conditioning of the matrix inversion that is involved in the computation of the $\mathscr{T}$ matrix,[26] i.e., the dimension of the matrix to be inverted (matrix [A] in Eq. (3.7) of Barber and Hill[25]) must be sufficiently large to compute accurately only a few leading elements of the inverse matrix.

As an example, in Table 1 the values of the parameters $n_{\max}^1$ and $n_{\max}^2$ are listed that provide the absolute accuracy $\Delta = 10^{-3}$ of computing the expansion coefficients a_1^2 to b_2^s. The data are given for Chebyshev particles, for which the notation $\mathrm{T}_n(\epsilon)$ is used,[24] and for spheroids, for which the notation $\mathrm{S}(d)$ is used, where ϵ is the deformation parameter and d is the ratio of the horizontal to rotational axes of the spheroid (note that $d > 1$ for oblate spheroids and $d < 1$ for prolate spheroids). For all the particles, the equal-volume-sphere size parameter is $x = 2\pi r/\lambda = 10$, where λ is the wavelength of light, and the index of refraction is $m_r = 1.5 + 0.02\,i$. Indeed, one sees from Table 1 that, depending on particle shape, the parameter $n_{\max}^2$ can be much smaller than $n_{\max}^1$.

To make use of this fact in practice, a good *a priori* estimate of the parameters $n_{\max}^1$ and $n_{\max}^2$ is needed. For axially symmetric scatterers, the $\mathscr{T}$-matrix $\mathbf{T}$ calculated in the body frame is decomposed into separate, independently calculated submatrices corresponding to different azimuthal modes m (see e.g., Chap. 5.4 of Ref. 10):

$$T_{mnmn'}^{ij} = \delta_{mm'} T_{mnmn'}^{ij}, \qquad |m| \leq n, n' \leq n_{\max}, \qquad i,j = 1, 2, \quad (17)$$

Tables 1. Parameters $n_{\max}^1$ and $n_{\max}^2$ for Chebyshev Particles and Spheroids With $m_r = 1.5 + 0.02\,i$, $x = 10$, and $\Delta = 10^{-3}$

Particle	$n_{\max}^1$	$n_{\max}^2$
$\mathrm{T}_2(-0.2)$	24	16
$\mathrm{T}_3(0.15)$	29	16
$\mathrm{T}_4(0.1)$	26	15
S(1/2)	26	19
S(1/3)	34	24
S(2)	22	17
S(3)	26	19

where δ_{ij} is the Kronecker delta. Therefore in real calculations it would be highly desirable to have a reliable estimate of $n_{\max}^1$ and $n_{\max}^2$ after computing only a single submatrix, preferably the zeroth one (because $T_{0n0n'}^{12} \equiv 0$ and $T_{0n0n'}^{21} \equiv 0$, computation of the zeroth submatrix requires much less time than computation of the first submatrix). After a lot of test calculations, we have found that the following simple convergence criterion can be used to determine $n_{\max}^1$:

$$\max\left[\left|\frac{C_1(n_{\max}^1) - C_1(n_{\max}^1 - 1)}{C_1(n_{\max}^1)}\right|, \left|\frac{C_2(n_{\max}^1) - C_2(n_{\max}^1 - 1)}{C_2(n_{\max}^1)}\right|\right] \leq 0.1\Delta, \quad (18)$$

where

$$C_1(n_{\max}) = -\frac{2\pi}{k^2}\,\mathrm{Re}\sum_{n=1}^{n_{\max}} (2n+1)(T_{0n0n}^{11} + T_{0n0n}^{22}), \quad (19)$$

$$C_2(n_{\max}) = \frac{2\pi}{k^2}\sum_{n=1}^{n_{\max}} (2n+1)[|T_{0n0n}^{11}|^2 + |T_{0n0n}^{22}|^2]; \quad (20)$$

$k = 2\pi/\lambda$ is the wavenumber and Δ is the desired absolute accuracy of computing the expansion coefficients a_1^s to b_2^s. After determining the parameter $n_{\max}^1$, the same zeroth $\mathscr{T}$ submatrix of the size $n_{\max}^1$ is used to determine the parameter $n_{\max}^2$ as the smallest positive integer satisfying the inequality

$$\max\left[\left|\frac{C_1(n_{\max}^2) - C_1(n_{\max}^1)}{C_1(n_{\max}^1)}\right|, \left|\frac{C_2(n_{\max}^2) - C_2(n_{\max}^1)}{C_2(n_{\max}^1)}\right|\right] \leq 0.1\Delta. \quad (21)$$

There is a natural motivation for using the quantities C_1 and C_2 in the convergence criterion. For randomly oriented axially symmetric particles, the orientationally averaged extinction and scattering cross sections are given by simple formulas[27]:

$$C_{\mathrm{ext}} = -\frac{2\pi}{k^2}\,\mathrm{Re}\sum_{n=1}^{n_{\max}}\sum_{m=-n}^{n} [T_{mnmn}^{11} + T_{mnmn}^{22}], \quad (22)$$

$$C_{\mathrm{sca}} = \frac{2\pi}{k^2}\sum_{n=1}^{n_{\max}}\sum_{n'=1}^{n_{\max}}\sum_{m=-\max(n,n')}^{\max(n,n')}\sum_{i,j=1,2} |T_{mnmn'}^{ij}|^2. \quad (23)$$

Equations (19) and (20) are obtained from Eqs. (22) and (23) by replacing the initial $\mathscr{T}$ matrix by a diagonalized matrix with elements $\delta_{m0}\delta_{nn'}\delta_{ij}T_{0n0n}^{ii}$. For spherical particles, $C_1 \equiv C_{\mathrm{ext}}$ and $C_2 \equiv C_{\mathrm{sca}}$ [see Eqs. (4.38)–(4.40) of Ref. 11], and the factor 0.1 in the right-hand side of Eq. (18) simply reflects the fact that for the same $n_{\max}^1$ and $n_{\max}^2$, the relative

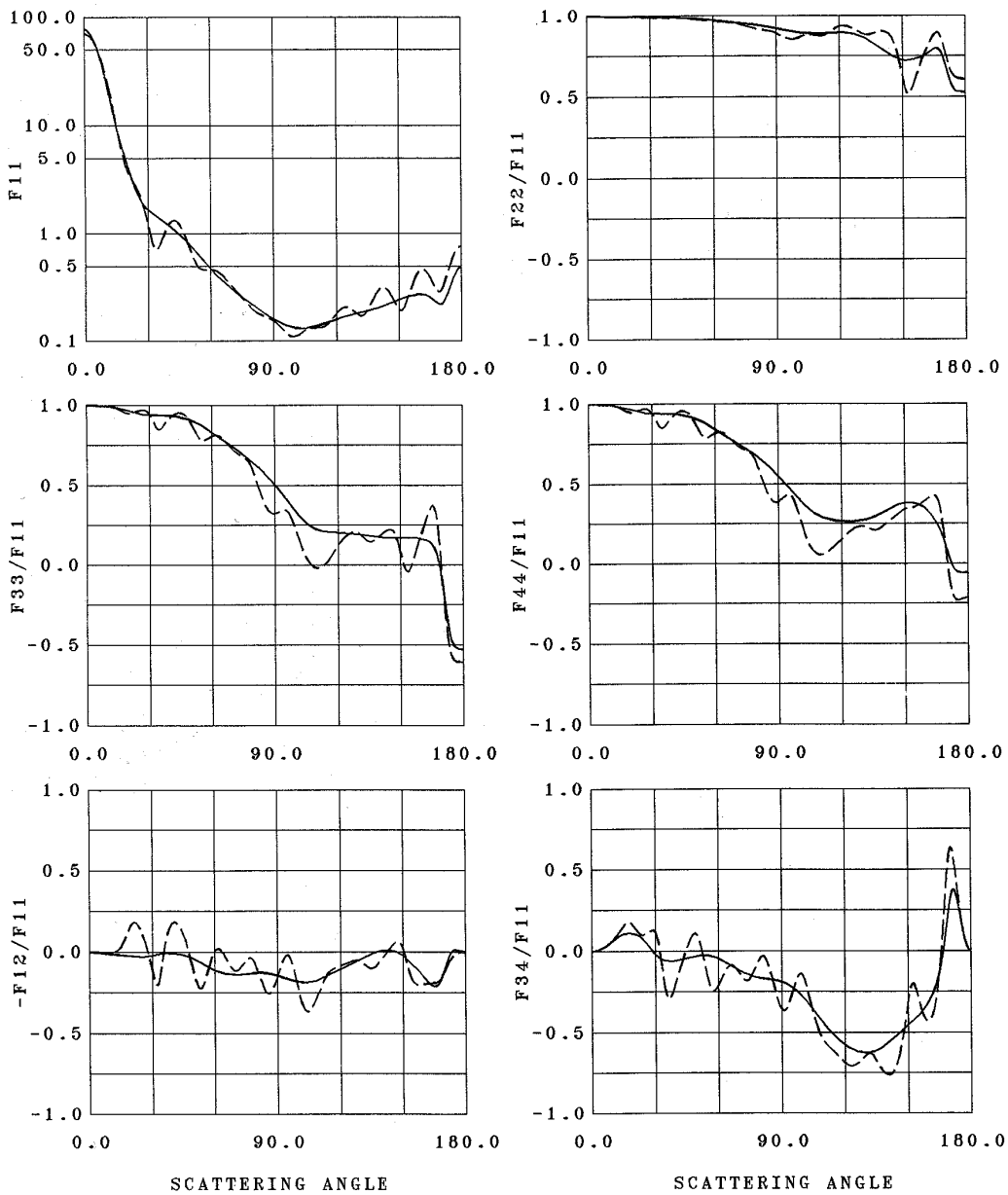

Fig. 1. Elements of the scattering matrix for a moderately wide power law size distribution of randomly oriented oblate spheroids with $d = 1.5$ and effective equal-volume-sphere radius $r_{\text{eff}} = 0.9102$ μm (solid curves) and randomly oriented monodisperse oblate spheroids with $d = 1.5$ and equal-volume-sphere radius $r = 0.9102$ μm (dashed curves).

accuracy of computing the optical cross sections is usually better than the absolute accuracy of computing the expansion coefficients by a factor of approximately 10. Although for nonspherical particles $C_1 \neq C_{\text{ext}}$ and $C_2 \neq C_{\text{sca}}$, the accuracy of computing these quantities provides a good estimate of the accuracy of computing the cross sections and expansion coefficients.

It was demonstrated in Ref. 11 that the analytical calculation of the orientationally averaged expansion coefficients a_1^s to b_2^s for a nonspherical particle required practically the same computer time as the calculation of the particle $\mathscr{T}$ matrix. The use of the fact that $n_{\max}^2$ is smaller than $n_{\max}^1$, and the fact that the two computer times are roughly proportional to the fourth power of $n_{\max}^2$ and $n_{\max}^1$, respectively, lead to a new conclusion: the calculation of the expansion coefficients is (much) less time consuming than the calculation of the $\mathscr{T}$ matrix. For example, for a Chebyshev particle $T_3(0.15)$ with $x = 10$, $m_r = 1.5 + 0.02\,i$, and $\Delta = 10^{-3}$, on an Amdahl 5870 computer the $\mathscr{T}$ matrix was computed in 29.4 s, whereas the expansion coefficients and the elements of the scattering matrix for 361 scattering angles were computed in

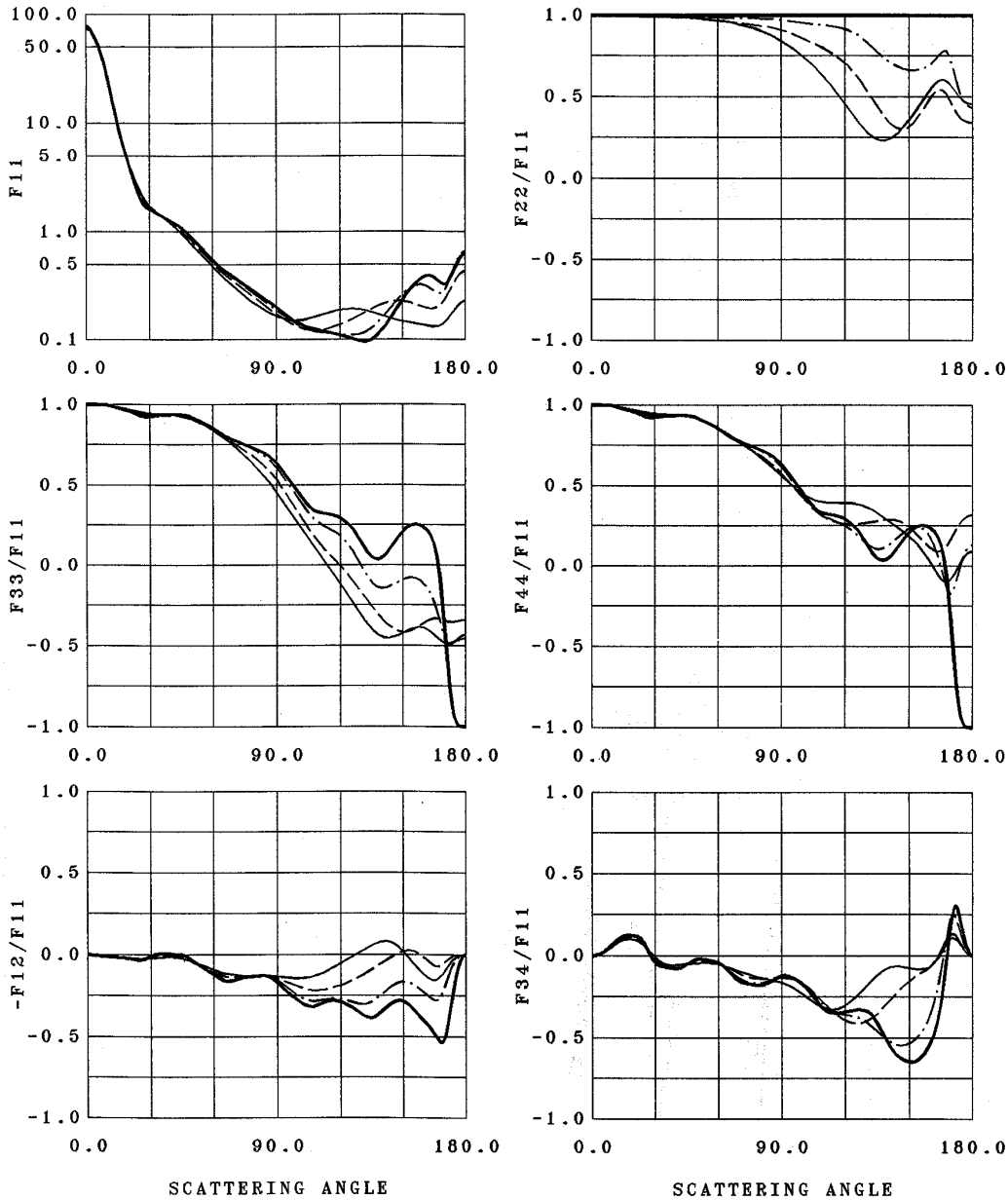

Fig. 2. Elements of the scattering matrix for the power law size distribution of prolate spheroids with $r_{min} = 0.5$ μm, $r_{max} = 1.5$ μm, and $d = 0.6$ (thin solid curves), 0.7 (dashed curves), and 0.83 (dotted-dashed curves), and for the same size distribution of spherical particles (thick solid curves).

4.8 s. Also, the $\mathscr{T}$-matrix elements are stored only for $|m|, n, n' \leq n_{max}^2$, which substantially reduces computer storage requirements.

B. Convergence Over m_{max}

Unlike Wiscombe and Mugnai[24] and Barber and Hill,[25] we do not check convergence of the $\mathscr{T}$-matrix computations over the parameter m_{max} (the largest azimuthal mode), but rather simply set $m_{max} = n_{max}^2$. It is interesting to note that for Chebyshev particles, the values of the parameter n_{max}^2 determined from Eq. (21) practically coincide with the values of m_{max} given in Table 1 of Wiscombe and Mugnai.[24]

C. Convergence Over N_G

Besides n_{max}, the accuracy of the $\mathscr{T}$-matrix computations depends also on the choice of the number of Gaussian quadrature points N_G used in computing surface integrals (see, e.g., Sec. 5 of Wiscombe and Mugnai[24] and Sec. 3.2 of Barber and Hill[25]). To

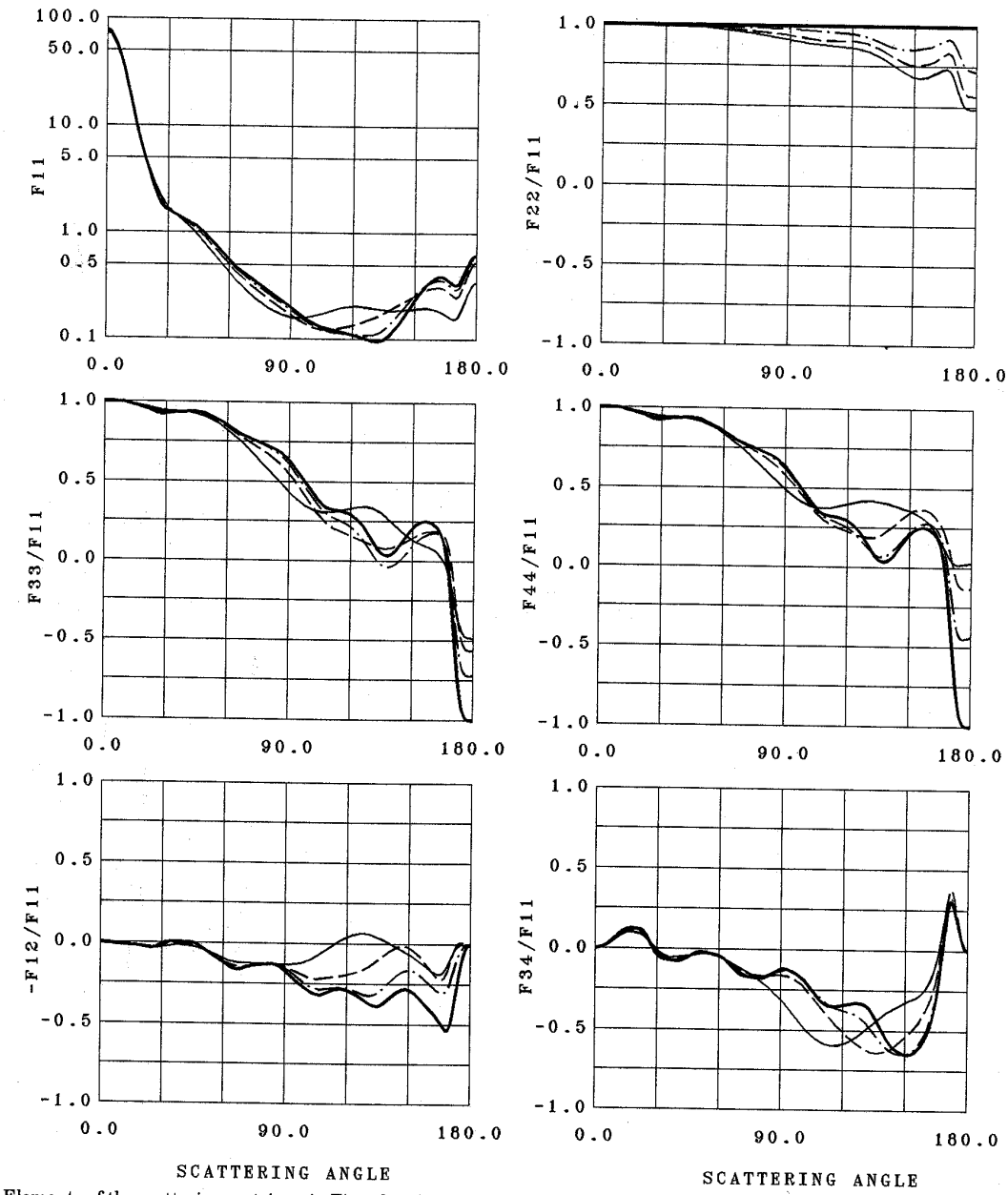

Fig. 3. Elements of the scattering matrix as in Fig. 2 but for oblate spheroids widh $d = 1.7$ (thin solid curves), 1.4 (dashed curves), and 1.2 (dotted-dashed curves).

check convergence over N_G, we use a procedure that is analogous to that of Barber and Hill.[25] Specifically, when determining the parameter $n_{\max}{}^1$, we set N_G equal to twice $n_{\max}{}^1$. After $n_{\max}{}^1$ has been determined, N_G is increased in steps of 4 until the quantities $C_1(n_{\max}{}^1)$ and $C_2(n_{\max}{}^1)$ converge within the relative accuracy $0.1\,\Delta$.

4. Calculations

In this section, we report and compare results of computer calculations for volume-equivalent spheroidal and spherical particles with the index of refraction $m_r = 1.5 + 0.02\,i$. This refractive index was adopted by Wiscombe and Mugnai[24] as typical of some maritime aerosols in the visible region. In all of the cases considered, the wavelength is $\lambda = 0.6283\ \mu\text{m}$, and the absolute accuracy of computing the expansion coefficients $a_1{}^s$ to $b_2{}^s$ is $\Delta = 10^{-3}$.

First in Fig. 1 the elements of the scattering matrix are plotted versus the angle of scattering for randomly oriented monodisperse oblate spheroids with $d = 1.5$ and equal-volume-sphere radius $r = 0.9102$

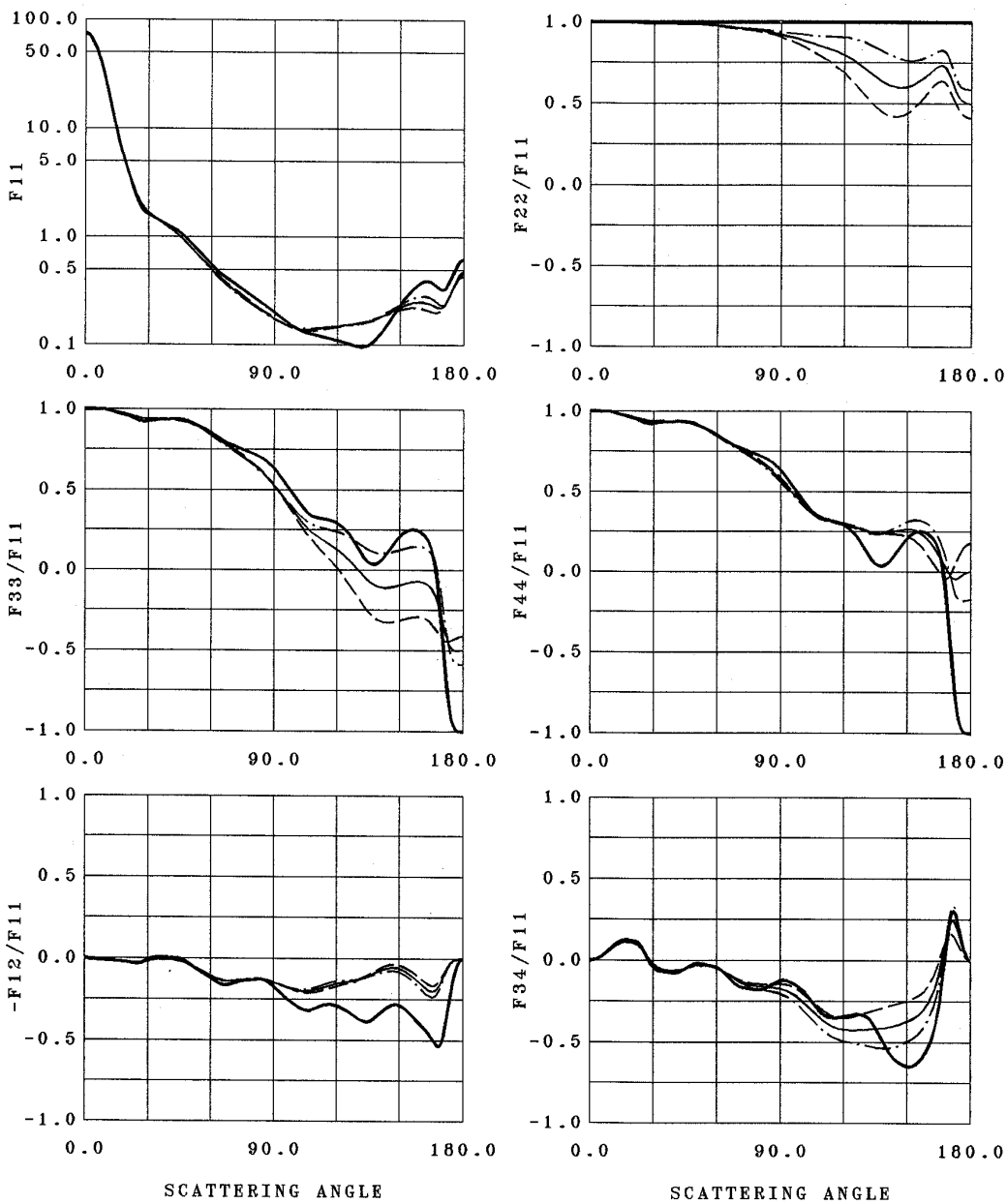

Fig. 4. Elements of the scattering matrix as in Fig. 2 but for shape averages over the prolate (dashed curves) and oblate (dotted-dashed curves) shapes, as well as the total averages over the six spheroidal shapes (thin solid curves).

μm and polydisperse spheroids with the same axes ratio and equal-volume-sphere radii governed by the power law distribution[28]

$$n(r) = \frac{2r_{\min}{}^2 r_{\max}{}^2}{r_{\max}{}^2 - r_{\min}{}^2} r^{-3}, \qquad r \in [r_{\min}, r_{\max}], \quad (24)$$

with $r_{\min} = 0.5$ μm and $r_{\max} = 1.5$ μm. For this size distribution, the effective equal-volume-sphere radius r_{eff}, as defined by Hansen and Travis,[28] is equal to the equal-volume-sphere radius of the monodisperse spheroids,

$$r_{\text{eff}} = \frac{r_{\max} - r_{\min}}{\ln(r_{\max}/r_{\min})} \approx 0.9102 \ \mu\text{m}, \quad (25)$$

and the effective variance is

$$\nu_{\text{eff}} = \frac{r_{\max} + r_{\min}}{2(r_{\max} - r_{\min})} \ln(r_{\max}/r_{\min}) - 1 \approx 0.0986. \quad (26)$$

Note that this value of the effective variance corre-

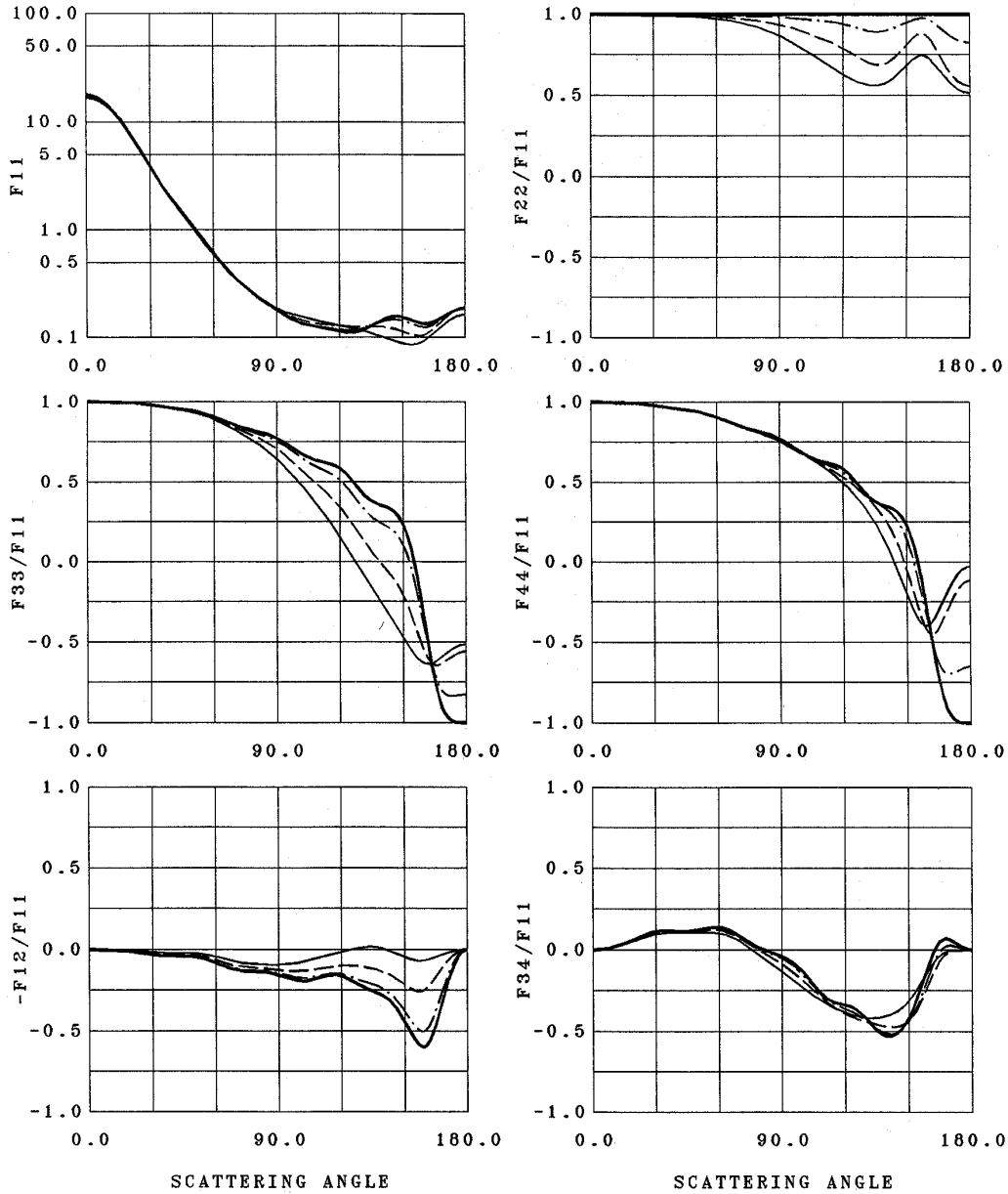

Fig. 5. Elements of the scattering matrix as in Fig. 2 but for smaller particles with $r_{min} = 0.2$ μm and $r_{max} = 0.6$ μm.

sponds to a moderately wide size distribution. It is seen from Fig. 1 that the elements of the scattering matrix for the polydispersion of moderately aspherical spheroids are much smoother than and differ substantially from those for the monodisperse particles. Thus, contrary to the expectation of Asano and Sato,[29] averaging the elements of the scattering matrix over orientations does not eliminate the necessity of averaging over particle sizes (see, also Chap. 2.5 of de Haan[2] and Chap. 2.4 of Stammes[30]).

In Fig. 2, numerical results are shown for polydisperse spherical particles and volume-equivalent prolate spheroids with $d = 0.6$, 0.7, and 0.83. The particle size distribution is given by Eq. (24), with $r_{min} = 0.5$ μm and $r_{max} = 1.5$ μm. Figure 3 is the same as Fig. 2 but for oblate spheroids, with $d = 1.7$, 1.4, and 1.2. In Figure 4, we show the shape-averaged results separately for the prolate and oblate spheroids, as well as the total averages over the six spheroidal shapes. For simplicity, in averaging over particle shapes we assumed that all the nonspherical shapes were equally probable [i.e., $p_j \equiv 1/J$ with $J = 6$ in Eqs. (10)–(13)]. Figures 5–7 are the same as Figs. 2–4 but for the power law distribution with

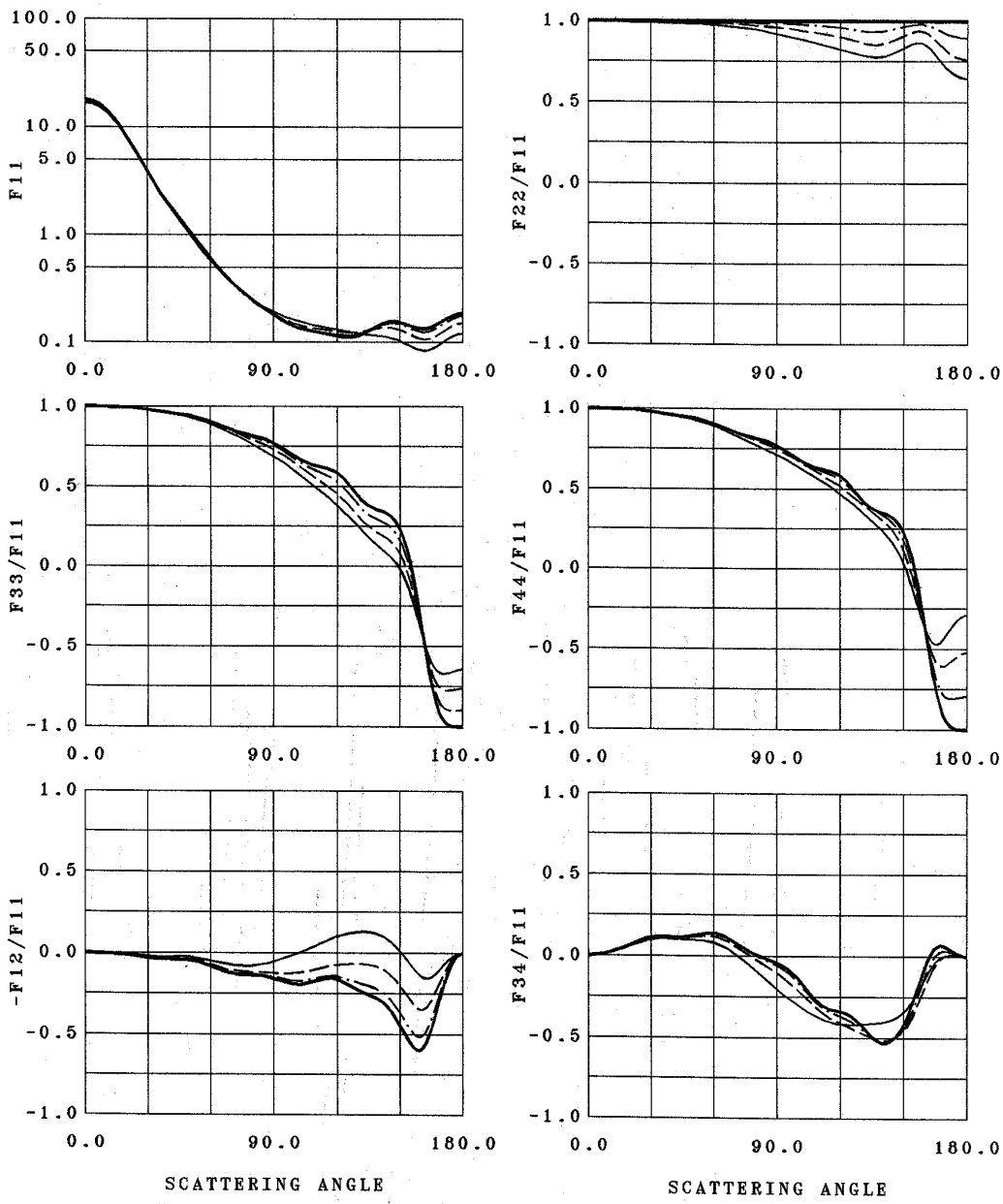

Fig. 6. Elements of the scattering matrix as in Fig. 3 but for the smaller particles.

r_{min} = 0.2 μm and r_{max} = 0.6 μm. Correspondingly the effective radius is now $r_{eff} \approx 0.3641$ μm, whereas the effective variance is the same: $\nu_{eff} \approx 0.0986$. In Tables 2 and 3, the corresponding values of the optical cross sections C_{sca}, C_{ext}, and C_{abs}, single-scattering albedo ϖ, and asymmetry parameter of the phase function g are given. Note that in calculating the integrals in Eqs. (10)–(13) numerically, we used 70 Gaussian division points for the bigger particles, with r_{min} = 0.5 μm and r_{max} = 1.5 μm and 20 points for the smaller particles, with r_{min} = 0.2 μm and r_{max} = 0.6 μm. The following conclusions can be drawn from the numerical data shown.

A. Intensity (F_{11})

The angular patterns of intensity are similar for volume-equivalent prolate and oblate spheroids of the same aspect ratio (the ratio of the largest to the smallest particle dimension). As compared with the equivalent spherical polydispersion, the size and size–shape distributions of the larger spheroids (Figs. 2–4) exhibit roughly the same forward scattering at scattering angles 0° to 30°, weaker side scattering at $\vartheta \in$ [30°, 100°], stronger side scattering at $\vartheta \in$ [100°, 150°], and weaker backscattering at $\vartheta \in$ [150°, 180°], which is in good agreement with the calculations of

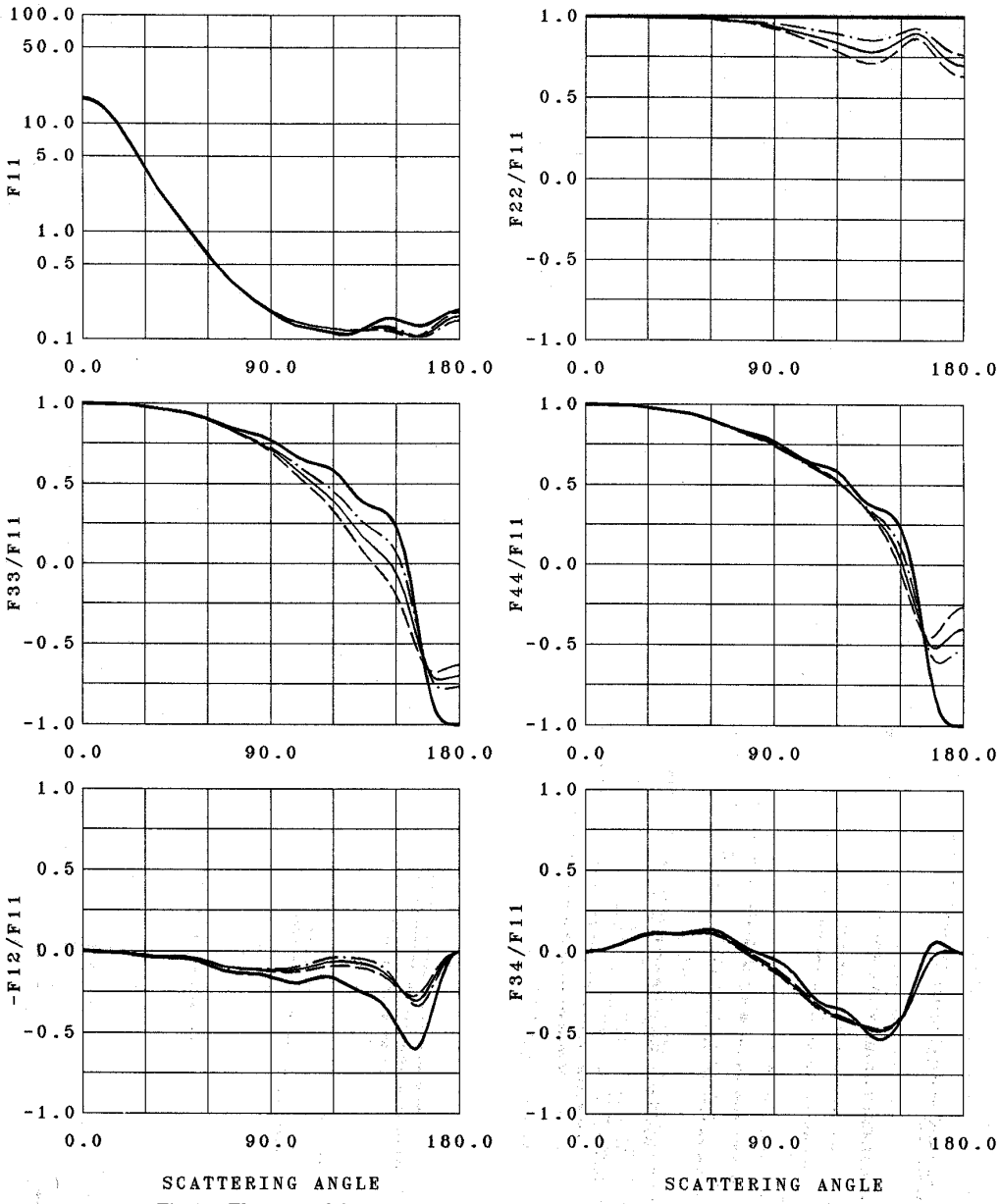

Fig. 7. Elements of the scattering matrix as in Fig. 4 but for the smaller particles.

Hill *et al.*[1] and the conclusions of Wiscombe and Mugnai.[3] The smaller spheroids (Figs. 5–7) do not differ from volume-equivalent spheres in the range [0°, 90°] and exhibit stronger side scattering at $\vartheta \in$ [90°, 135°] and weaker backscattering at $\vartheta \in$ [135°, 180°].

B. F_{22}/F_{11}

Although for spheres $F_{22}/F_{11} \equiv 1$, for spheroidal particles this ratio strongly depends on particle asphericity and can substantially deviate from unity. The deviation is smaller for oblate spheroids than for prolate spheroids with the same aspect ratio, the oblate–prolate difference being larger for the larger particles. For all the nonspherical particles, the ratio has a minimum near 135–150° and a maximum near 160–165° (cf. Stammes[30]).

C. F_{33}/F_{11} and F_{44}/F_{11}

Unlike spherical particles, for all the spheroidal shapes $F_{33}/F_{11} \neq F_{44}/F_{11}$, the ratio F_{44}/F_{11} being larger than F_{33}/F_{11} (cf. Ref. 30). For oblate spheroids, F_{33}/F_{11} is closer to F_{44}/F_{11} than for prolate spheroids of the same aspect ratio, which is in agreement with the

Table 2. Optical Cross Sections for Scattering C_{sca}, Extinction C_{ext}, and Absorption C_{abs}, Albedo for Single Scattering ϖ, and Asymmetry Parameter of the Phase Function g for Polydisperse Spheres and Size and Size–Shape Distributions of Volume Equivalent Spheroids With $r_{min} = 0.5$ μm and $r_{max} = 1.5$ μm

Particles	C_{sca}[a]	C_{ext}[a]	C_{abs}[a]	ϖ	g
S(0.6)	3.950	5.211	1.261	0.758	0.761
S(0.7)	3.781	5.035	1.254	0.751	0.752
S(0.83)	3.661	4.905	1.244	0.746	0.748
S(1.7)	4.012	5.277	1.265	0.760	0.754
S(1.4)	3.776	5.030	1.254	0.751	0.748
S(1.2)	3.661	4.905	1.244	0.746	0.747
⟨Prolate⟩[b]	3.797	5.050	1.253	0.752	0.754
⟨Oblate⟩[c]	3.816	5.071	1.254	0.753	0.750
⟨Total⟩[d]	3.807	5.060	1.254	0.752	0.752
Spheres	3.615	4.853	1.238	0.745	0.747

[a]In square micrometers.
[b]Average over all prolate spheroids.
[c]Average over all oblate spheroids.
[d]Average all over all spheroids.

general inequality[31]

$$|F_{33} - F_{44}| \leq F_{11} - F_{22} \tag{27}$$

(cf. Refs. 29, 30, and 32).

D. Linear Polarization $(-F_{12}/F_{11})$

As in the case of intensity, angular patterns of linear polarization are similar for volume-equivalent prolate and oblate spheroids of the same aspect ratio. As is seen from Figs. 8 and 9, as aspect ratio increases linear polarization tends to be positive at a wider range of scattering angles (cf. Refs. 29 and 30), and prolate–oblate differences become more pronounced.

E. F_{34}/F_{11}

For the smaller particles, this ratio is practically independent of particle shape. However, this is not observed for the bigger particles, for which F_{34}/F_{11} is different for the oblate and prolate spheroids and spheres at scattering angles greater than 60°.

F. Optical Cross Sections, Single-Scattering Albedo, and Asymmetry Parameter

As is seen from Table 2, for the size–shape distributions of the larger spheroids the optical cross sections for scattering C_{sca}, extinction C_{ext}, and absorption C_{abs}, single-scattering albedo, ϖ, and asymmetry parameter of the phase function g are systematically greater than those of the volume-equivalent spherical polydispersion. However, as follows from Tables 2 and 3, for the moderately aspherical particles spherical–nonspherical differences are not large.

5. Concluding Remarks

In this paper, we have described a computational scheme for rigorously calculating the light scattering by size–shape distributions of randomly oriented axially symmetric particles of a size comparable to a wavelength. This scheme is based on the $\mathcal{T}$-matrix method, as extended to randomly oriented scatterers in our recent paper,[11] and a newly developed conver-

Table 3. Optical Cross Sections for Scattering, C_{sca}, Extinction, C_{ext}, and Absorption, C_{abs}, Albedo for Single Scattering ϖ, and Asymmetry Parameter of the Phase Function g for $r_{min} = 0.2$ μm and $r_{max} = 0.6$ μm

Particles	C_{sca}[a]	C_{ext}[a]	C_{abs}[a]	ϖ	g
S(0.6)	0.915	1.014	0.099	0.902	0.750
S(0.7)	0.911	1.011	0.099	0.902	0.744
S(0.83)	0.909	1.008	0.099	0.901	0.740
S(1.7)	0.908	1.007	0.099	0.902	0.749
S(1.4)	0.909	1.008	0.099	0.902	0.743
S(1.2)	0.909	1.008	0.099	0.901	0.740
⟨Prolate⟩[b]	0.912	1.011	0.099	0.902	0.745
⟨Oblate⟩[c]	0.909	1.008	0.099	0.902	0.744
⟨Total⟩[d]	0.910	1.009	0.099	0.902	0.744
Spheres	0.908	1.008	0.100	0.901	0.739

[a]In square micrometers.
[b]Average over all prolate spheroids.
[c]Average over all oblate spheroids.
[d]Average all over all spheroids.

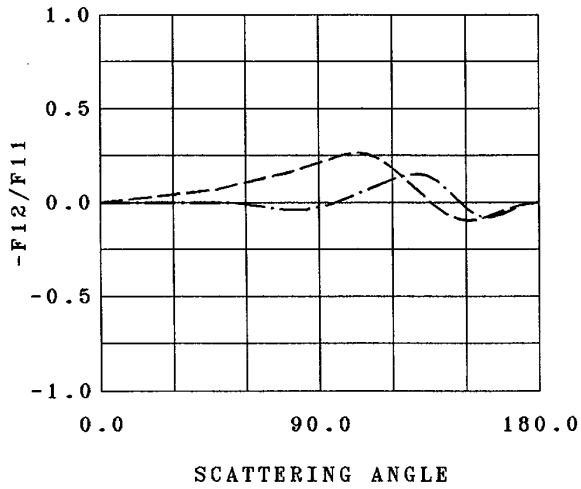

Fig. 8. Linear polarization $-F_{12}/F_{11}$ for the power law size distribution of randomly oriented prolate spheroids with $r_{min} = 0.2$ μm, $r_{max} = 0.6$ μm, and $d = 1/3$ (dashed curve) and 1/2 (dotted-dashed curve).

gence procedure that takes into account particular features of the $\mathcal{T}$-matrix approach, is especially suitable to the case of randomly oriented particles, and enables one to reduce substantially computer time and storage requirements. The computational scheme described is efficient and allows the use of moderate computers. For example, the calculation of the curves displayed in Fig. 3 required only 40 CPU minutes on an Amdahl 5870 computer, which is rated at a speed of approximately 24 million instructions per second, although this calculation included computations for 210 different nonspherical particles with equal-volume-sphere size parameters up to 15.

In a sense, our computational scheme resembles the statistical approach outlined by Bohren and Singham.[6] Indeed, we do not calculate separately the elements of the scattering matrix for all possible particle sizes, shapes, and orientations. Instead, the ensemble-averaged expansion coefficients a_1^s to b_2^s are calculated and are then used in calculations of either single or multiple light scattering. Moreover, the orientational averaging step is completely avoided by using the analytical method developed in Ref. 11. The only difference is that our approach is based on the $\mathcal{T}$-matrix method instead of the coupled-dipole method,[33,34] as proposed by Bohren and Singham.[6]

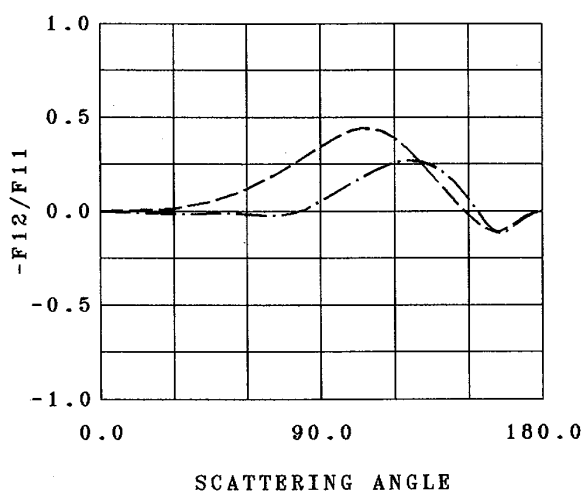

Fig. 9. Linear polarization as in Fig. 8 but for oblate spheroids with $d = 3$ (dashed curve) and 2 (dotted–dashed curve).

To model the scatter of particle sizes in real ensembles, we used a moderately wide power law distribution of equal-volume-sphere radii and demonstrated the necessity of macro-size averaging to make nonspherical scattering curves sufficiently smooth and representative. We have presented and discussed results of computer calculations for volume-equivalent polydispersions of spheres and size–shape distributions of moderately aspherical prolate and oblate spheroids with the index of refraction $1.5 + 0.02\,i$. Like many other investigators that used theoretical or experimental techniques to study various aspects of nonspherical scattering (see, e.g., Refs. 1–6, 29, 30, 32, and 35–37), we have found that the angular behavior of the elements of the scattering matrix for nonspherical particles differs significantly from that of the scattering matrix for equivalent spherical particles. In particular, the size and size–shape distributions of spheroids exhibit stronger side scattering near 120° and weaker backscattering, the ratio F_{22}/F_{11} of the elements of the scattering matrix substantially deviates from unity, and the element F_{33} is greatly different from F_{44}. For size distributions of volume-equivalent oblate and prolate spheroids of the same aspect ratio, the ratios F_{22}/F_{11}, F_{33}/F_{11}, and F_{34}/F_{11} can differ substantially and, thus, are indicators of particle shape, whereas the angular patterns of the intensity (F_{11}) and linear polarization ($-F_{12}/F_{11}$) are similar. With increasing asphericity of oblate and prolate spheroids, linear polarization tends to be positive at a wider range of scattering angles. For all the nonspherical cases considered, the ratio F_{44}/F_{11} is larger than F_{33}/F_{11}. For oblate spheroids, the ratio F_{22}/F_{11} is closer to unity and F_{33}/F_{11} is closer to F_{44}/F_{11} than for volume-equivalent prolate spheroids of the same aspect ratio. For the size–shape distributions of moderately aspherical spheroids, the optical cross sections, single-scattering albedo, and asymmetry parameter of the phase function do not differ substantially from those of the volume-equivalent spheres. In general, as is seen from Figs. 2–7 and Tables 2 and 3, all the light-scattering characteristics are more shape-dependent for larger particles.

Finally we note that although in this paper we compared light-scattering properties of volume-equivalent particles, some authors prefer to define particle equivalence in terms of equal surface area or equal averaged projected area (for randomly oriented convex particles these two definitions are identical[38]).

Equal-volume spheres are usually regarded as the best replacement for nonspherical particles smaller than the wavelength, because in this case scattering depends primarily on particle volume, not particle surface area. On the other hand, equal-projected-area spheres are generally accepted as a proper substitute for nonspherical particles much bigger than the wavelength, because the diffraction intensity peak depends primarily on the averaged projected area. To make our study more complete, we repeated all our calculations assuming that r in Eqs. (10)–(13) and (24) was the radius of the equal-projected-area sphere. However, because the particles considered were only moderately nonspherical and had sizes of the order of the wavelength, the results of these calculations were close to those shown in Figs. 2–7 and Tables 2 and 3. Therefore we were unable to conclude what definition of particle equivalence should be preferred.

The author is indebted to J. Hansen, L. Travis, B. Carlson, M. Sato, and E. Yanovitskij for valuable discussions and to F. Kuik and an anonymous reviewer for useful comments on a preliminary version of this paper. I also gratefully acknowledge programming support from A. Wolf and A. Walker.

References

1. S. C. Hill, A. C. Hill, and P. W. Barber, "Light scattering by size/shape distributions of soil particles and spheroids," Appl. Opt. **23,** 1025–1031 (1984).
2. J. F. de Haan, "Effects of aerosols on the brightness and polarization of cloudless planetary atmospheres," Ph.D. dissertation (Free University, Amsterdam, 1987).
3. W. J. Wiscombe and A. Mugnai, "Scattering from nonspherical Chebyshev particles. 2. Means of angular scattering patterns," Appl. Opt. **27,** 2405–2421 (1988).
4. M. I. Mishchenko, "Infrared absorption by shape distributions of NH_3 ice particles: an application to the Jovian atmosphere," Earth Moon Planet **53,** 149–156 (1991).
5. F. Kuik, J. F. de Haan, and J. W. Hovenier, "Benchmark results for single scattering by spheroids," J. Quant. Spectrosc. Radiat. Transfer **47,** 477–489 (1992).
6. C. F. Bohren and S. B. Singham, "Backscattering by nonspherical particles: a review of methods and suggested new approaches," J. Geophys. Res. D **96,** 5269–5277 (1991).
7. P. C. Waterman, "Symmetry, unitarity, and geometry in electromagnetic scattering," Phys. Rev. D **3,** 825–839 (1971); "Matrix methods in potential theory and electromagnetic scattering," J. Appl. Phys. **50,** 4550–4566 (1979); B. Peterson and S. Ström, "T matrix for electromagnetic scattering from an arbitrary number of scatterers and representations of $E(3)$," Phys. Rev. D **8,** 3661–3678 (1973).
8. P. Barber and C. Yeh, "Scattering of electromagnetic waves by arbitrarily shaped dielectric bodies," Appl. Opt. **14,** 2864–2872 (1975); D.-S. Wang and P. W. Barber, "Scattering by inhomogeneous nonspherical objects," Appl. Opt. **18,** 1190–1197 (1979).
9. V. K. Varadan and V. V. Varadan, eds., *Acoustic, Electromagnetic and Elastic Wave Scattering—Focus on the T-Matrix Approach* (Pergamon, New York, 1980).
10. L. Tsang, J. A. Kong, and R. T. Shin, *Theory of Microwave Remote Sensing* (Wiley, New York, 1985).
11. M. I. Mishchenko, "Light scattering by randomly oriented axially symmetric particles," J. Opt. Soc. Am. A **8,** 871–882 (1991).
12. H. C. van de Hulst, *Light Scattering by Small Particles* (Wiley, New York, 1957).
13. C. F. Bohren and D. R. Huffman, *Absorption and Scattering of Light by Small Particles* (Wiley, New York, 1983).
14. I. Kuščer and M. Ribarič, "Matrix formalism in the theory of diffusion of light," Opt. Acta **6,** 42–51 (1959).
15. H. Domke, "The expansion of scattering matrices for an isotropic medium in generalized spherical functions," Astrophys. Space Sci. **29,** 379–386 (1974); "Fourier expansion of the phase matrix for Mie scattering," Z. Meteorol. **25,** 357–361 (1975); O. I. Bugaenko, "Generalized spherical functions in the Mie problem," Izv. Atmos. Oceanic Phys. **12,** 366–370 (1976).
16. C. E. Siewert, "On the equation of transfer relevant to the scattering of polarized light," Astrophys. J. **245,** 1080–1086 (1981); "On the phase matrix basic to the scattering of polarized light," Astron. Astrophys. **109,** 195–200 (1982).
17. J. W. Hovenier and C. V. M. van der Mee, "Fundamental relationships relevant to the transfer of polarized light in a scattering atmosphere," Astron. Astrophys. **128,** 1–16 (1983); C. V. M. van der Mee and J. W. Hovenier, "Expansion coefficients in polarized light transfer," Astron. Astrophys. **228,** 559–568 (1990).
18. I. M. Gelfand, R. A. Minlos, and Z. Ya. Shapiro, *Representations of the Rotation and Lorentz Groups and Their Applications* (Pergamon, Oxford, 1963).
19. J. F. de Haan, P. B. Bosma, and J. W. Hovenier, "The adding method for multiple scattering calculations of polarized light," Astron. Astrophys. **183,** 371–391 (1987); P. Stammes, J. F. de Haan, and J. W. Hovenier, "The polarized internal radiation field of a planetary atmosphere," Astron. Astrophys. **225,** 239–259 (1989).
20. R. D. M. Garcia and C. E. Siewert, "A generalized spherical harmonics solution for radiative transfer models that include polarization effects," J. Quant. Spectrosc. Radiat. Transfer **36,** 401–423 (1986); "The F_N method for radiative transfer models that include polarization effects," J. Quant. Spectrosc. Radiat. Transfer **41,** 117–145 (1989).
21. M. I. Mishchenko, "The fast invariant imbedding method for polarized light: computational aspects and numerical results for Rayleigh scattering," J. Quant. Spectrosc. Radiat. Transfer **43,** 163–171 (1990); "Reflection of polarized light by plane-parallel slabs containing randomly-oriented, nonspherical particles," J. Quant. Spectrosc. Radiat. Transfer **46,** 171–181 (1991).
22. W. M. F. Wauben and J. W. Hovenier, "Polarized radiation of an atmosphere containing randomly-oriented spheroids," J. Quant. Spectrosc. Radiat. Transfer **47,** 491–504 (1992).
23. P. W. Barber, "Differential scattering of electromagnetic waves by homogeneous isotropic dielectric bodies," Ph.D. dissertation (University of California, Los Angeles, Los Angeles, Calif. 1973).
24. W. J. Wiscombe and A. Mugnai, "Single scattering from nonspherical Chebyshev particles: a compendium of calculations," NASA Ref. Publ. 1157 (Goddard Space Flight Center, National Aeronautics and Space Administration, Greenbelt, Md., 1986).
25. P. W. Barber and S. C. Hill, *Light Scattering by Particles: Computational Methods* (World Scientific, Singapore, 1990).
26. P. W. Barber, "Resonance electromagnetic absorption by nonspherical dielectric objects," IEEE Trans. Microwave Theory Tech. **MTT-25,** 373–381 (1977).
27. M. I. Mishchenko, "Interstellar light absorption by randomly oriented nonspherical dust grains," Sov. Astron. Lett. **15,** 299–302 (1989); "Extinction of light by randomly-oriented nonspherical grains," Astrophys. Space Sci. **164,** 1–13 (1990); "Calculation of the total optical cross sections for an ensemble

of randomly oriented nonspherical particles," Kinem. Fiz. Nebes. Tel **6**(5), 95–96 (1990); N. G. Khlebtsov, "Orientational averaging of light scattering observables in the $\mathscr{F}$-matrix approach," Appl. Opt. **31,** 5359–5365 (1992).
28. J. E. Hansen and L. D. Travis, "Light scattering in planetary atmospheres," Space Sci. Rev. **16,** 527–610 (1974).
29. S. Asano and M. Sato, "Light scattering by randomly oriented spheroidal particles," Appl. Opt. **19,** 962–974 (1980).
30. P. Stammes, "Light scattering properties of aerosols and the radiation inside a planetary atmosphere," Ph.D. dissertation (Free University, Amsterdam, 1989).
31. E. S. Fry and G. W. Kattawar, "Relationships between elements of the Stokes matrix," Appl. Opt. **20,** 2811 (1981); J. W. Hovenier, H. C. van de Hulst, and C. V. M. van der Mee, "Conditions for the elements of the scattering matrix," Astron. Astrophys. **157,** 301 (1986).
32. R. J. Perry, A. J. Hant, and D. R. Huffman, "Experimental determinations of Mueller scattering matrices for nonspherical particles," Appl. Opt. **17,** 2700–2710 (1978).
33. W. M. McClain and W. A. Ghoul, "Elastic light scattering by randomly oriented macromolecules: computation of the complete set of observables," J. Chem. Phys. **84,** 6609–6622 (1986).
34. M. K. Singham, S. B. Singham, and G. C. Salzman, "The scattering matrix for randomly oriented particles," J. Chem. Phys. **85,** 3807–3815 (1986).
35. A. C. Holland and G. Gagne, "The scattering of polarized light by polydisperse systems of irregular particles," Appl. Opt. **9,** 1113–1121 (1970).
36. R. H. Zerull, "Scattering measurements of dielectric and absorbing nonspherical particles," Beitr. Phys. Atmos. **49,** 168–188 (1976).
37. D. L. Jaggard, C. Hill, R. W. Shorthill, D. Stuart, M. Glantz, F. Rosswog, B. Taggart, and S. Hammond, "Light scattering from particles of regular and irregular shape," Atmos. Environ. **15,** 2511–2519 (1981).
38. V. Vouk, "Projected area of convex bodies," Nature (London) **162,** 330–331 (1948).